

Alkyl- and arylsilsesquiazanes: effect of the R group on polymer degradation and ceramic char composition

GARY T. BURNS, TIMOTHY P. ANGELOTTI, LARRY F. HANNEMAN,
GRISH CHANDRA, JOHN A. MOORE
Dow Corning Corporation, Midland, Michigan 48686-0995, USA

A series of alkyl- and arylsilsesquiazanes $[\text{RSi}(\text{NH})_{3/2}]$ was prepared by the ammonolysis of the corresponding RSiCl_3 . Each polymer was pyrolysed to 1200°C in an inert atmosphere to give amorphous Si–C–N ceramic chars. The major volatile products in the pyrolysis effluent were identified and quantified by a combination of TGA–GCMS, TGA–GCFTIR and pyrolysis–capillary GC techniques. Mechanistic aspects correlating the alkyl/aryl group on the polymer structure, decomposition and ceramic char composition were studied. Oxidative stability of the ceramic chars fits percolation theory. The oxygen contents of ceramic chars containing ≤ 25 wt% carbon increased 1 to 2% after 12 h at 1200°C . At higher levels of carbon the chars were completely oxidized to SiO_2 .

1. Introduction

The utilization of organosilicon compounds as precursors to high-strength Si–C–N–O structural ceramics is a rapidly developing field. Interest in this approach was sparked by the reports of Verbeeck, Winter and Mansmann [1–3] in the early 1970s who reported the production of small diameter ceramic fibres from polymeric carbosilazanes. Although this approach was never commercialized and eventually abandoned, research into the use of silazanes and carbosilazanes as ceramic precursors has continued worldwide. In the last ten years, several reports have appeared describing the production of preceramic polymers based on the reaction of di- and trichlorosilanes with hexamethyldisilazane [4–7], ammonia [8, 9] and primary alkyl amines [10]. When heated to high temperatures ($> 1000^\circ\text{C}$) in an inert atmosphere, these polymers have been reported to yield ceramic chars consisting of silicon, carbon, nitrogen and oxygen in varying ratios and microstructure, depending upon the polymer composition and firing conditions used. Unfortunately, although a wide variety of alkyl substituents on silicon is claimed in many of the reports, few, if any, details are given relating the effect of changing the alkyl group on polymer and ceramic properties.

In order to ascertain the above effects, two series of R groups were evaluated. In the first series (R = methyl, ethyl, isopropyl, phenyl, benzyl, allyl and t-butyl), the R group was varied such that homolytic cleavage of the Si–C bond during pyrolysis would produce a silyl radical and either a primary, substituted primary, secondary, phenyl, benzylic, allylic or a tertiary carbon radical, respectively. In the second series (R = ethyl, propyl, isobutyl, 3-butenyl, 2-phenethyl and 2-methylphenethyl) the R group was varied such that alpha C–C bond cleavage would produce an SiC^\cdot radical and either a primary, sub-

stituted primary, secondary, allylic, benzylic or a secondary benzylic carbon radical. By comparing the pyrolysis products of the two series, the initial point of cleavage (i.e. Si–C or C–C) and mode of decomposition (radical compared to a concerted β elimination) were determined. We report herein, the effect of the alkyl substituent in a series of silsesquiazanes $[\text{RSi}(\text{NH})_{3/2}]$ on polymer properties, mode of polymer degradation during pyrolysis, ceramic char composition and the oxidative stability of the ceramic chars.

2. Experimental procedure

2.1. Polymer synthesis and characterization

Numerous reports and experimental procedures for the preparation of silsesquiazane polymers from trichlorosilanes exist in the literature (for a partial review see Wills *et al.* [11]). The polymers reported here were prepared from a composite procedure in which the RSiCl_3 was dissolved in 7 to 10 volumes of toluene, the toluene solution cooled to below -30°C (limited dry ice/acetone) and anhydrous ammonia rapidly bubbled through the solution for 1 to 2 h. The soluble fraction was isolated by warming the reaction mixture to room temperature, filtering it through diatomaceous earth and evaporating the volatiles from the filtrate under reduced pressure (all manipulations were performed in an inert, dry atmosphere). The isolated polymers ranged from brittle resins to low viscosity oils depending upon the R group. Each of the polymers was characterized by a combination of elemental analysis, gel permeation chromatography (GPC), thermal mechanical (TMA) and thermogravimetric (TGA) analyses and infrared and ^1H NMR spectroscopy. Portions of these data are summarized in Table I.

2.2. Polymer pyrolysis

The volatile gases produced during polymer pyrolysis

TABLE I Polymer characterization

Polymer	Yield (%)	Molecular weight			Char yield		
		M_w	M_n	Dispersion	TGA (1000° C)	Furnace (1200° C)	TMA
R = Methyl	16	2 778	486	5.7	65	62	84.4
Ethyl	65	2 318	846	3.6	39	17	37
Propyl	72	19 063	2013	9.5	22	7.6	—
Isopropyl	79	1 769	1095	1.6	16	7.2	—
Isobutyl	85	3 525	2097	1.7	23	13	73
t-Butyl	27	—	—	—	—	9.1	—
Allyl	78	13 724	1646	8.1	71	61	—
3-Butenyl	53	—	—	—	—	58	—
Phenyl	85	1 924	927	2.1	64	47	105.5
Benzyl	72	2 009	1071	1.9	39	17	67.3
Phenethyl	86	3 612	1838	2.0	50	65	—
2-Methylphenethyl	95	839	536	1.6	33	47	—
2-Trimethylsilylethyl	72	764	400	1.9	36	5.5	—

were identified and quantified in a two-step process. In the first step, 100 to 200 mg polymer was placed in a DuPont model 701 TGA and pyrolysed to 1000° C (helium atmosphere) using a temperature programme of 20° C min⁻¹ from room temperature to 300° C, 5° C min⁻¹ from 300 to 700° C and 20° C min⁻¹ from 700 to 1000° C. Aliquots of the pyrolysis effluent were sampled on-line every 50° C between 300 and 700° C with a gas-tight syringe and injected into a model 4610 Finnigan GCMS (70 eV, electron impact, 30 m SPB-1 column). In addition, the total effluent was collected in a U-tube trap cooled to -196° C. Upon warming the trap to room temperature, aliquots were injected into a model 60SX Nicolet GC-FTIR and the Finnigan GCMS. The products were identified by comparison of their mass and infrared spectra with those of authentic samples.

In the second step, the pyrolysis products were generated and quantitated using a Pyroprobe^R 122 interfaced to a Varian 3700 gas chromatograph equipped with a capillary inlet splitter, cryogenic oven cooling and a flame ionization detector; the chromatographic data were acquired and processed by a Perkin Elmer Model 3230 Chromatographic Laboratory Automation System. The necessary separations were achieved using a 60 m × 0.25 mm DB-1 (0.25 μm film thickness) fused silica capillary column (J & W Scientific, Inc.). Column oven temperature programmes and mobile phase linear velocities were adjusted to provide the required resolutions in a minimum of time. Identification of the analytes was achieved by comparison of pyrolysis chromatograms with the elution profiles obtained in the gas chromatography/mass spectrometry experiment described above, retention measurements of standard compounds or use of Kovats Retention Indices.

Quantitative measurements were made using an internal standard approach and substance specific relative response factors. The flame ionization detector response factors used for these measurements are of the form of the substance-specific correction factor described by Kaiser [12]. This factor is the number by which the area of the peak must be multiplied for the corrected area to be directly proportional to the weight of the substance. A simple approximation of the substance-specific correction factor reported by

Onkiehong [13] has been used in this work:

$$R_f = M_i/12n$$

where R_f is the substance-specific correction factor for substance i , M_i the molecular weight of substance i , n the number of carbon atoms in substance i . A standard solution of n -octadecane (~ 3% wt/wt) in n -pentadecane was accurately prepared.

The sample and an aliquot of the standard solution were weighed into a quartz pyrolysis boat and the boat inserted in the standard ¼ in. diameter Pyroprobe^R Coil Probe. With the helium mobile phase off and gas chromatographic Pyroprobe^R interface at ambient temperature, the probe and sample were inserted and sealed in the interface. The mobile phase was set to the appropriate pressure and the interface brought to operating temperature (280° C) while holding the column oven at 0° C. The volatilized solvent and standard were deposited on the head of the column during this period. Once the system was up to operating conditions, the column oven temperature programme was initiated and a chromatogram of the standard obtained. Throughout the study the area per unit weight of standard was monitored to define precision of the approach.

After obtaining the internal standard chromatogram, the column oven was set to the appropriate temperature, the initial pyrolysis temperature set and the pyrolysis gas chromatogram obtained. Using a predefined pyrolysis sequence, pyrolysis temperatures were increased stepwise and chromatograms obtained at each temperature. Quantitative measurements were obtained of each analyte at each pyrolysis temperature by relating the adjusted peak areas to the adjusted peak area of the internal standard.

2.3. Preparation of ceramic chars/evaluation of oxidative stabilities

Aliquots of 1 to 10 g of each polymer were fired in a three-zone 2 in. Lindberg tube furnace to 1200° C at 5° C min⁻¹ with a 2 h hold at 1200° C in an argon atmosphere. After cooling to ambient temperature under an argon atmosphere, the samples were removed and weighed. Portions of each ceramic char were ground to a fine powder (average particle size of 40 to 60 μm). Samples of each char both before and

TABLE II Bond strengths [16]

Me ₃ Si-CH ₃	89.4	C-N	66
Me ₃ Si-NHMe	100	N-H	92
Me ₃ SiCH ₂ -H	99		
Me ₃ SiCHCH ₃	95		
H			
CH ₃ -H	105	CH ₃ -CH ₃	88
MeCH ₂ -H	98	C ₂ H ₅ -CH ₃	85
Me ₂ CH-H	95	Me ₂ CH-CH ₃	84
Me ₃ C-H	92	Me ₃ C-CH ₃	82
PhCH ₂ -H	88		

after grinding were then weighed into alumina boats and heated at 5°C min⁻¹ to 1200°C and held at 1200°C for 12 h in an atmosphere of either ambient or dry air; after cooling to room temperature, the oxidized chars were analysed for oxygen content using a model R0136 LECO oxygen analyser. Similar results were obtained in both ambient and dry air atmospheres.

3. Results and discussion

3.1. Effect of the alkyl group on polymer properties

Table I summarizes the pertinent polymer characterization data. The effect of the R group on polymer morphology and stability is a function of the R group's steric size and potential cross-linking sites. The stability of an uncondensed primary silylamine (RSiNH₂) increases as the size of the R group increases. Hence, in the case where R = methyl, insufficient steric bulk is present during ammonolysis; this results in a low yield of soluble polymer (i.e. high gel yield). At the other extreme, when R = t-butyl a very high yield of soluble material is obtained. However, in this case, sufficient steric bulk is present such that the product is incompletely condensed and still contains a large amount of primary silylamines (see Fig. 1). As a result, the product is primarily a low molecular weight oligomer which distills during the vacuum drying step; the overall polymer yield is quite low. In all of the other cases, a sufficient trade-off between the R group's steric bulk and silylamine con-

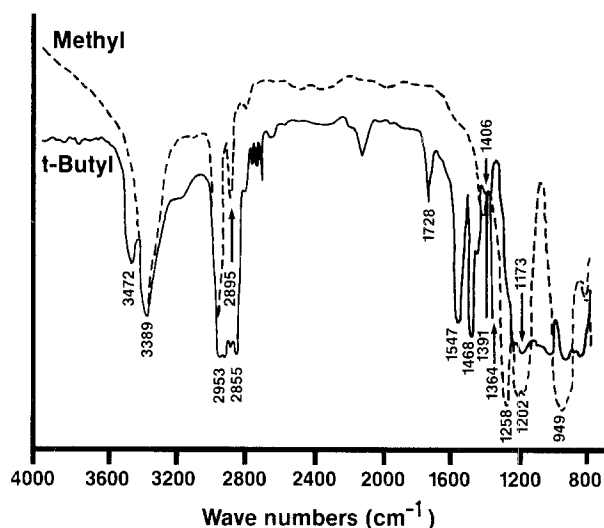


Figure 1 Comparison of methyl and t-butyl SQZ.

densation is achieved; high yields of soluble materials are obtained. Unfortunately, the data in Table I do not show the differences in the thermal stabilities of the polymer. Several of the polymers "drifted" at room temperature, changing from soluble, tacky resins to cross-linked gums after a few days or weeks. Similar observations have been reported for other silsesquiazanes. For example, see Liviu and Haiduc [14] and Zhinkin *et al.* [15]. Consequently, the molecular weights recorded for many of the polymers were more a function of when the data were taken and not of the steric bulk of the R group. In general, the most stable polymers are those containing isobutyl, phenyl and benzyl R groups.

3.2. Mechanism of polymer degradation

All of the silsesquiazanes contain only five types of single bonds, namely Si-C, Si-N, C-C, C-H and N-H bonds. Of these, the silicon-carbon and the carbon-carbon bonds are the weakest bonds and are approximately the same strength (89.4 kcal mol⁻¹ for tetramethylsilane compared to 88 kcal mol⁻¹ for ethane) (see Table II). (The values shown in Table II

TABLE III Polymer pyrolysis*

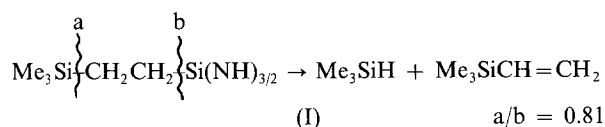
RSi(NH) _{3/2}	Product (% yield)	
R = Me	CH ₄ (29) [†]	-
Et	CH ₂ =CH ₂ (20)	-
Propyl	CH ₃ CH=CH ₂ (12.5)	CH ₄ (4.1)
Isopropyl	CH ₃ CH=CH ₂ (35.1)	CH ₄ (14.8)
Isobutyl	(Me) ₂ C=CH ₂ (20.3)	CH ₃ CH=CH ₂ (3.2)
	CH ₄ (2.8)	-
t-butyl	(Me) ₂ C=CH ₂ (5.1)	CH ₃ CH=CH ₂ (1.0)
	CH ₄ (1.3)	-
Allyl	CH ₃ CH=CH ₂ (29)	CH ₄ (43.5)
3-Butenyl	H ₂ C=C(H)-C(H)=CH ₂	CH ₃ CH=CH ₂
Phenyl	Ph-H(50.8)	-
Benzyl	PhCH ₃ (12.0)	Ph-H(6.5)
Phenethyl	PhCH=CH ₂ (64.7)	PhCH ₃ (5.7)
	PhH(5.9)	CH ₂ =CH ₂ (6.4)
2-Methylphenethyl	PhCH=CH ₂ (16.7)	PhCH ₃ (0.3)
	PhH(1.4)	CH ₂ =CH ₂ (1.6)
Me ₃ SiCH ₂ CH ₂	Me ₃ SiH(2.5)	Me ₃ SiH(2.1)
	CH ₂ =CH ₂ (0.7)	-

*Products were identified by a combination of GC-FTIR and GCMS.

[†] Yields are absolute. Ammonia and oligomers were not identified.

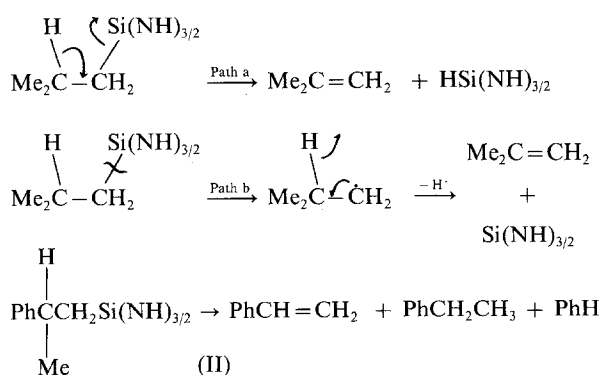
were taken from Walsh [16].) However, carbon-carbon bond strengths are highly substituent dependent and follow the trends of carbon radical stability. Hence, the carbon-carbon bond in neopentane is weaker than the carbon-carbon bond in ethane (82 kcal mol⁻¹ cf. 88 kcal mol⁻¹). Although data are unavailable, a similar trend would be expected for silicon-carbon bond strengths. As such, by varying the nature of the R group, the initial point of cleavage (i.e. Si-C or alpha C-C) should be dependent upon the nature of the R group. The results of the pyrolysis study are summarized in Table III.

To assess the effect of nitrogen substitution on silicon on the silicon-carbon bond strengths, the initial R group investigated was 2-trimethylsilylethyl. In this group, two points of silicon-carbon cleavage are possible, a and b (Scheme I). Pyrolysis of 2-trimethylsilylethylsilsesquiazane gave products, trimethylsilane (a) and trimethylvinylsilane (b), arising from both points in an a/b ratio of 0.81. Therefore, the effect of nitrogen is to favour Si-C bond cleavage. In fact, in every case but one, the major product is the alkene corresponding to silicon-carbon bond cleavage. The one exception occurs when R = 2-methylphenethyl where cleavage of the alpha carbon-carbon bond results in a secondary benzylic radical.



Further insight into the mode of initial polymer decomposition can be gleaned by comparing the pyrolysis products of R = 2-methylphenethyl and R = isobutyl. Alkene elimination from the polymer can be envisioned in either of two ways (Scheme II): a concerted β Si-H elimination (path a) or a radical process involving an initial Si-C bond homolysis to give a carbon radical which generates the alkene in a subsequent β H elimination (path b). Both pathways predict isobutene as the major product when R = isobutyl. However, for R = 2-methylphenethyl, path a predicts alpha-methylstyrene, which was not detected, as the major product. The major product, styrene, results from cleavage of the weaker carbon-carbon bond implying a radical process such as shown in path b.

In at least two cases it appears that the major pyrolysis product undergoes a secondary decomposition to



two new products. Examination of the pyrolysis products from R = isobutyl and R = t-butyl shows a remarkable similarity amongst the products and product ratios. For example, the product ratio of isobutene to propene is 6.0 for R = isobutyl and 5.1 for R = t-butyl. This, in combination with nearly identical yields of propene and methane in each case, suggests that, under the reaction conditions, isobutene undergoes a secondary decomposition to propene and methane. A similar situation occurs with styrene which appears to undergo further decomposition to benzene and ethylene. In both cases where it is a pyrolysis product, R = phenethyl and R = 2-methylphenethyl, benzene and ethylene are formed in nearly identical yields and ratios to styrene (10.1 and 10.4, respectively).

3.3. Effect of the R group on ceramic char composition

The effect of the R group on ceramic char composition can be seen by examining the elemental analysis data for the chars summarized in Table IV. On the basis of per cent carbon in the ceramic chars, the R groups readily divide themselves into two groups, saturated and unsaturated. All of the saturated alkyl groups tested gave ceramic chars containing 9 to 15 wt% carbon, regardless of structure and number of carbon atoms (methyl, ethyl, propyl and isobutyl). In contrast, unsaturated R groups gave ceramic chars with both higher carbon contents and a greater range (23 to 56%). In general, increasing the number of carbon atoms in an unsaturated R group increased the amount of carbon in the char. Thus, the per cent carbon in the chars followed the trend allyl < 3-butenyl < phenyl < benzyl. Likewise, a series of methyl/phenyl copolymers followed this trend: increasing the mole per cent of phenyl in the copolymer and, hence, the amount of unsaturation, increased the amount of carbon in the char. However, both 2-methylphenethyl and vinylsilsesquiazane failed to follow this trend. In the case of vinylsilsesquiazane a char with a higher than expected carbon content was obtained, while 2-methylphenethyl gave a lower than expected carbon content. In addition to the previously described series of alkylsilsesquiazanes, several additional copolymers (phenyl/methyl) and a vinylsilsesquiazane were prepared and charred to 1200°C according to the procedures described in Sections 2.1 and 2.2. The additional data were primarily used to broaden the investigation on the effect of the R group on ceramic char composition (Section 3.3) and the effect on a ceramic char's oxidative stability.

All of the ceramic chars were analysed by X-ray diffraction techniques and found to be amorphous.

3.4. Effect of carbon on the oxidative stability of Si-C-N ceramics

The effect of the R group on a ceramics' oxidative stability is directly related to the carbon content that the R group imparts to its char. This is summarized in Table V and Figs 2 and 3. Fig. 2 shows the effect of carbon for unground ceramic chars. In this case, little to no deterioration in the ceramics' oxidative

TABLE IV Ceramic characterization

RSi(NH) _{3/2}	Elemental composition of 1200° C, argon ceramics				Density
	Silicon	Carbon	Nitrogen	Oxygen	
R = Methyl	56.6	9.2	30.4	1.7	2.21
Ethyl	51.9	14.6	27.4	4.2	2.19
Propyl	50.8	13.4	24.6	2.3	< 1.91
Isobutyl	52.6	14.2	29.2	2.42	2.19
Allyl	43.6	23.2	30	0.49	< 1.91
3-Butenyl	44.3	25.5	22.4	6.4	—
Phenyl	31.7	47.9	17.7	1.7	< 1.91
Benzyl	24.6	55.7	12.4	1.9	< 1.91
2-Methylphenethyl	35.5	40.5	18.8	1.0	< 1.91
Vinyl	41.4	28.0	27.4	1.7	—
Phenyl/methyl (20/80)	47.9	22.5	26.6	1.1	—
Phenyl/methyl (30/70)	42.4	25.8	26.5	0.64	—
Phenyl/methyl (40/60)	42.6	27.7	21.8	1.1	—
Phenyl/methyl (45/55)	42.0	30.6	24.3	0.81	—
Phenyl/methyl (50/50)	40.4	34.1	23.7	1.19	—
Phenyl/methyl (55/45)	40.1	34.6	23.0	0.94	—
Phenyl/methyl (60/40)	36.3	36.0	22.3	1.26	—
Phenyl/methyl (70/30)	31.8	40.6	20.9	1.1	—
Phenyl/methyl (80/20)	34.1	42.5	19.9	0.99	—

resistance occurs until the carbon content of the char reaches 35 to 40 wt %. At this point, the oxidation resistance of the char fails catastrophically and the samples are completely oxidized to silica. Increasing the effective surface area by grinding the char (average particle size 40 to 60 μm) results in a similar curve (see Fig. 3); however, the location of the baseline and the phase transition where oxidative failure occurs differ.

Both the differences between the two curves and the existence of a sharp phase transition where oxidation resistance is lost can be explained by a combination of surface area and percolation theory. An amorphous SiCN ceramic char can be thought of as SiCN and C domains randomly dispersed in space [17]. As long as the amount of carbon is relatively low, i.e. the SiCN is a continuous phase, a surface oxide forms (e.g. [18]) on the SiCN phase preventing further oxidation of both the carbon and the SiCN domains. As the weight per cent of carbon increases, the size of these SiCN domains decreases, and at some point the carbon

becomes a continuous phase. At this point oxygen can "percolate" through the matrix resulting in a complete loss of oxidative resistance. For unground chars, this phase transition occurs between 35 and 40 wt % carbon. By grinding the ceramic char (average particle size 40 to 60 μm), the effective surface area is increased. Consequently, the percolation transition shifts to a lower weight per cent of carbon and the baseline is raised.

4. Conclusions

A series of silsesquiazane polymers were prepared by the total ammonolysis of the corresponding RSiCl₃. Within the series the R group was varied to give insight on the effect of the R group on polymer morphology, mechanism of thermal decomposition and ceramic composition. Several general conclusions can be drawn concerning the above points.

1. Silsesquiazanes thermally degrade by a two-step radical mechanism involving an initial silicon-carbon bond cleavage followed by a β elimination of a

TABLE V Change in % oxygen after oxidation

Silsesquiazane	wt % carbon (1200° C, argon)	% oxygen (1200° C, air)	
		unground	ground
Methyl	9.2	0.53	14.2
Ethyl	14.6	1.76	—
Propyl	13.4	1.7	—
Isobutyl	14.2	1.5	35.1
Allyl	23.0	0.6	37.1
Phenyl	47.9	51.2	51.4
Benzyl	55.7	51.5	—
2-Methylphenethyl	40.5	40.4	—
Phenyl/methyl (20/80)	22.5	1.1	43.5
Phenyl/methyl (30/70)	25.8	0.3	49.2
Phenyl/methyl (40/60)	27.7	1.2	41.7
Phenyl/methyl (45/55)	30.6	1.1	50.3
Phenyl/methyl (50/50)	34.1	4.9	49.3
Phenyl/methyl (55/45)	34.6	5.5	49.8
Phenyl/methyl (60/40)	36	2.5	50.3
Phenyl/methyl (70/30)	40.6	15.8	51.7
Phenyl/methyl (80/20)	42.5	15.6	50.2

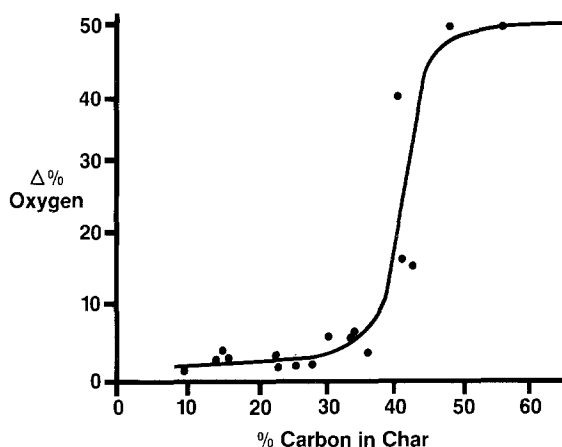


Figure 2 Oxidative stability of unground chars.

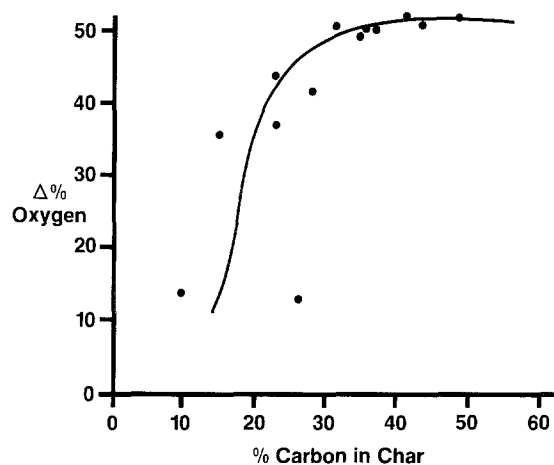


Figure 3 Oxidative stability of ground chars.

hydrogen radical.

2. Saturated alkyl groups contribute approximately the same amount of carbon to a ceramic char independent of the alkyl group structure.

3. The carbon content in a ceramic char derived from an unsaturated R group increases as the number of carbons in the R group increase.

4. The oxidative stability of an amorphous Si-C-N ceramic char is a function of surface area and carbon content in accordance with percolation theory predictions. For unground ceramic chars, this phase transition occurs at approximately 35 to 40 wt % carbon.

Although no single R group satisfied all the needs for the synthesis of the penultimate preceramic polymer for mixed Si-C-N ceramics, several of the R groups imposed severe limitations on the designers of these polymers. In particular, the aryl groups introduce the problems of large amounts of excess carbon and the loss of oxidative resistance.

References

1. W. VERBEEK, *Ger. Offen.* 2218960 (1973).
2. W. VERBEEK and G. WINTER, *Ger. Offen.* 2236078 (1974).
3. G. WINTER, W. VERBEEK and M. MANSMANN, *Ger. Offen.* 2243527 (1974).
4. J. H. GAUL Jr, US Patent 4312970 (1982).
5. J. P. CANNADY, US Patent 4540803, September (1985).
6. *Idem*, US Patent 4543344, September (1985).
7. J. H. GAUL Jr, US Patent 4340619, July (1982).
8. D. SEYFERTH, G. H. WISEMAN and C. PRUD'HOMME, *J. Amer. Ceram. Soc.* **66** (1983) C13.
9. V. A. MAZAEV, L. PODOBEDA and A. YA. KOROLEV, *Poroshk. Metall.* (1978) 91.
10. D. SEYFERTH and G. H. WISEMAN, *Commun. Amer. Ceram. Soc.* (1984) C132.
11. R. R. WILLS, R. A. MARKLE and S. P. MUKHERJEE, *Ceram. Bull.* **62** (1983) 904.
12. R. KAISER, "Gas Phase Chromatography" (Butterworths, London, 1963).
13. L. ONKIEHONG, "Gas Phase Chromatography 1960" (Butterworths, London, 1960) p. 7.
14. V. LIVIU and I. HAIDUC, *Stud. Univ. BabeşBolyai, Ser. Chem.* **15** (1970) 45.
15. D. YA. ZHINKIN, G. M. MAL'NOVA and ZH. V. GORISLAVSKAYA, *Obshch. Khim.* **37** (1967) 2124.
16. R. WALSH, *Acc. Chem. Res.* **14** (1981) 246.
17. J. LIPOWITZ, H. A. FREEMAN, H. A. GOLDBERG, R. T. CHEN and E. R. PRACK, *J. Amer. Ceram. Soc.*, submitted.
18. D. W. RICHERSON, "Modern Ceramic Engineering" (Marcel Dekker, New York, 1982) p. 117.

Received 3 September
and accepted 12 November 1986